ACS Chemical Neuroscience

Research Article

pubs.acs.org/chemneuro

Direct Correlation of Cell Toxicity to Conformational Ensembles of Genetic Aβ Variants

Arun Kumar Somavarapu and Kasper P. Kepp*

DTU Chemistry, Technical University of Denmark, Kemiorvet 206, DK-2800 Kongens Lyngby, Denmark

Supporting Information

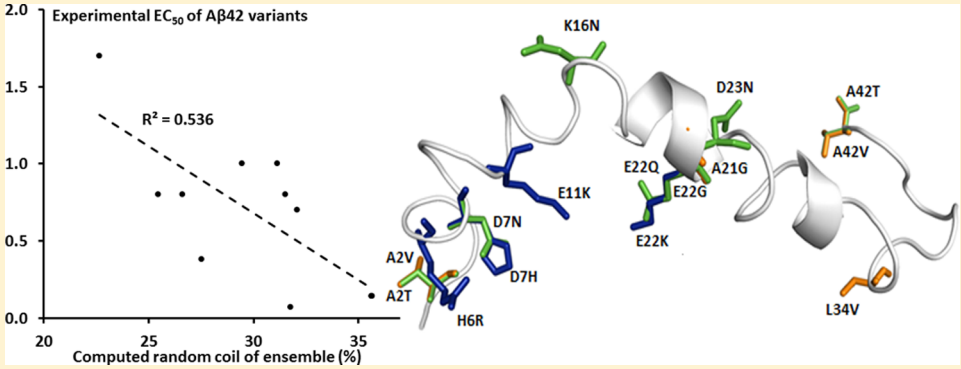

ABSTRACT: We report a systematic analysis of conformational ensembles generated from multiseed molecular dynamics simulations of all 15 known genetic variants of $A\beta_{42}$. We show that experimentally determined variant toxicities are largely explained by random coil content of the amyloid ensembles (correlation with smaller EC_{50} values; $R^2 = 0.54$, $p = 0.01$), and to some extent the helix character (more helix-character is less toxic, $R^2 = 0.32$, $p = 0.07$) and hydrophobic surface ($R^2 = 0.37$, $p = 0.04$). Our findings suggest that qualitative structural features of the amyloids, rather than the quantitative levels, are fundamentally related to neurodegeneration. The data provide molecular explanations for the high toxicity of E22 variants and for the protective features of the recently characterized A2T variant. The identified conformational features, for example, the local helix−coil-strand transitions of the C-terminals of the peptides, are of likely interest in the direct targeting of amyloids by rational drug design.

KEYWORDS: *Amyloid beta, Alzheimer's disease, structural ensembles, toxicity, coil*

Alzheimer's disease (AD) is a major neurodegenerative disease causing loss of cognitive skills, difficulty in problem solving, and changes in behavior and identity.[1,2] Deposits of post-translationally modified β-sheet aggregates consisting of amyloid beta (Aβ) outside neurons and of tau protein inside neurons are two of the main pathological features of AD.[3] The Aβ peptides vary in length, with the $A\beta_{42}$ isoform being particularly toxic.[4,5] Aβ peptides are produced from the transmembrane amyloid precursor protein (APP) upon proteolysis by the combination of β- and γ-secretases.[6,7] The Aβ peptides also accumulate inside neurons as soluble oligomers, which are now perceived to be the pathogenic forms of Aβ[8−10] and thus desirable targets for next-generation Alzheimer drugs.[11,12]

More than 30 mutations have been reported in APP: 15 missense point mutations have been identified in humans within the $A\beta_{42}$ region of APP (672−713), as shown in Figure 1A. Of these, the Flemish (A21G),[13] Arctic (E22G),[14] Italian (E22K),[15] Dutch (E22Q),[16] and Iowa (D23N)[17] mutations occur in the middle of the Aβ sequence close to the α-cleavage site that leads to nonamyloidogenic cleavage of APP. Mutations at E22 and D23 lead to substantially more toxic and aggregation-prone Aβ variants in cell assays.[18,19] The English (H6R),[20] Taiwanese (D7H),[21] and Tottori (D7N)[22] mutations occur in the hydrophilic N-terminal part of the peptide and cause early onset familial AD (FAD). These mutants are also substantially more aggregation-prone than wild-type Aβ.[21,23] Both monomers[24] and dimers[25,26] are present in humans,[27] and monomers have been associated with possible protective normal functions.[28] Yet, under certain conditions, these forms can undergo conformational changes into β-strand-containing oligomers, and eventually to β-sheet-rich fibrils.[29−31] The genetic variants have been shown to affect Aβ dynamics and monomer folding and oligomerization.[32,33]

The A2T[34] and A2V[35] mutations at the second position of Aβ are of particular interest, since A2T has been shown to be protective against AD; it also reduces β-secretase cleavage of APP.[36] A2T-overexpressing human neurons revealed reduced aggregation consistent with a protective effect,[37] that is, both changes in steady-state levels and long−short isoform ratios

Received: September 8, 2015
Accepted: October 7, 2015
Published: October 8, 2015

DOI: 10.1021/acschemneuro.5b00238
ACS Chem. Neurosci. 2015, 6, 1990−1996

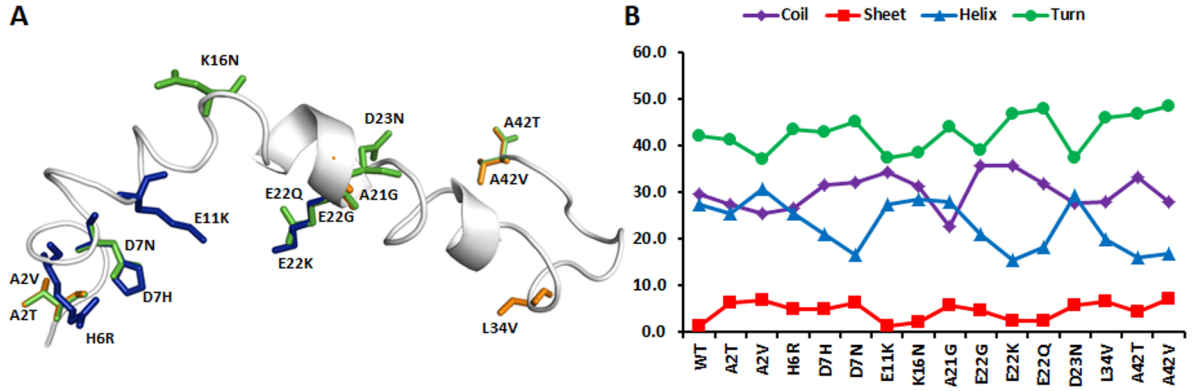

Figure 1. (A) Wild-type and mutant structures of Aβ_{42} shown in stick format; blue refers to positively charged, green to polar uncharged, and orange refers to hydrophobic. (B) Percentage of secondary structure for all Aβ variants assigned according to the DSSP algorithm.

and specific chemical properties of the produced variant may be involved: Which one is more important is not yet known. Interestingly, in contrast the A2V variant is pathogenic in the homozygous state.[38]

The Piedmont variant (L34V) causes severe cerebral amyloid angiopathy (CAA) without amyloid plaques or neurofibrillary tangles.[39] The E11K mutation causes early onset FAD and affects β-cleavage.[40,41] The mutation K16N occurs at the α-secretase cleavage site which likely interrupts this cleavage activity and results in higher quantities of Aβ, but is also resistant toward Aβ-degradation by neprilysin,[42] again illustrating how genetic variants can affect both APP processing and thereby, steady-state amyloid levels and ratios (the "quantitative" effect), and the chemical properties of the produced variant Aβ (the "qualitative" effect). The A42T mutation occurs at the γ-secretase cleavage site and gives rise to late-onset Alzheimer's disease with cerebrovascular lesions.[43−45]

We used multiseed molecular dynamics (MD) simulations of all known missense point mutations in Aβ_{42} to systematically pinpoint structural and chemical features that may contribute to toxicity of these variants. Realistic monomer ensembles are central to recent efforts that screen for Aβ-targeting compounds.[46,47] Since structural ensembles and properties can be quite method-dependent,[48] it is important to study the variants in their totality. This first complete comparison of Aβ variants shows that simple, specific conformational features of the variant ensembles correlate strongly to the variant's toxicity and thus that amyloid toxicity is very much a qualitative (conformational and chemical) rather than quantitative (steady-state levels) feature of amyloids.

RESULTS AND DISCUSSION

For each variant, four independent simulations were performed to improve sampling; backbone RMSD graphs can be found in Supporting Information, Figure S1. The RMSDs gradually increased up to typically 20 ns of simulation time and then stayed at 6−12 Å and displayed horizontal RMSD plots in most cases. The large RMSDs are consistent with expectations and previous observations of these highly disordered peptides.[49−51] It is also expected that the peptides will visit several conformational basins in phase space. Several transitions are observed in some of the variants and in the wild type during simulation, showing why multiple simulations are necessary for each variant. The properties that we discuss are averaged over the last 20−100 ns of all four simulations for each Aβ variant.

Not all the amyloid variants have been previously investigated, and experimental NMR structures have only been reported for the wild type. Our systematic simulations thus enable the first complete comparison of the structural ensembles of all variants and the first statistical correlation to experimental toxicities. Figure 1B shows the secondary structure content for each Aβ_{42} variant, derived using Amber99sb-ILDN in explicit water, known to have a realistic secondary-structure balance.[52−54]

In general, our simulations reveal a tendency toward turns and coil in all Aβ_{42} variants. In comparison to the wild type, the variants of the C-terminal region (L34 V, A42T, and A42V) and the Italian (E22K) and Dutch (E22Q) mutants have considerably more turn character. All mutants except E11K showed increased β-strand character, with the most strand-prone variants being A42V, A2V, Piedmont (L34 V), Tottori (D7N), and A2T (6−7% strand character). The starting structure of Aβ_{42} from an NMR experiment in a water-*co*-solvent mixture had 36% helix character. Helix character decreased in all variants during simulation, consistent with the simulations occurring in 100% water, which reduces helix content and increases coil: For comparison, the NMR structure of the related Aβ_{40} isoform in pure water, 2LFM,[55] has ∼25% helix and more coil than other NMR structures deposited in the PDB, consistent with our ensembles. This structure has been successfully used to screen for Aβ-targeting compounds,[46,47] and properties of FAD mutations mapped on this ensemble correlate with FAD patient age of onset.[56] Other NMR structures of Aβ, such as 1IYT[57] and 1BA4,[58] have more helix character because the experiments were conducted in less polar environments (micelles and cosolvents) where helix dipoles are stabilized; this is, incidentally, also why helices tend to be favored in membranes. In the variants D7N, E22K, E22Q, L34 V, A42T, and A42V, helix character was <18%. The numerical data of this analysis are in the Supporting Information, Table S1.

The secondary-structure propensity of each residue of each Aβ variant is shown in Supporting Information Figures S2 (A2T to K16N) and S3 (A21G to A42V). Wild-type Aβ_{42} has four segments with substantial helix propensity (blue), 2−5, 11−18, 23−28, and 36−38 and has almost no strand character (red). Many of the variants (in fact, all except E22K) have tendencies to strand formation in the C-terminal, hydrophobic part of the peptides supposedly involved in oligomerization. It is notable that helix character is particularly low and coil/turn character particularly high for E22 variants known exper-

DOI: 10.1021/acschemneuro.5b00238
ACS Chem. Neurosci. 2015, 6, 1990−1996

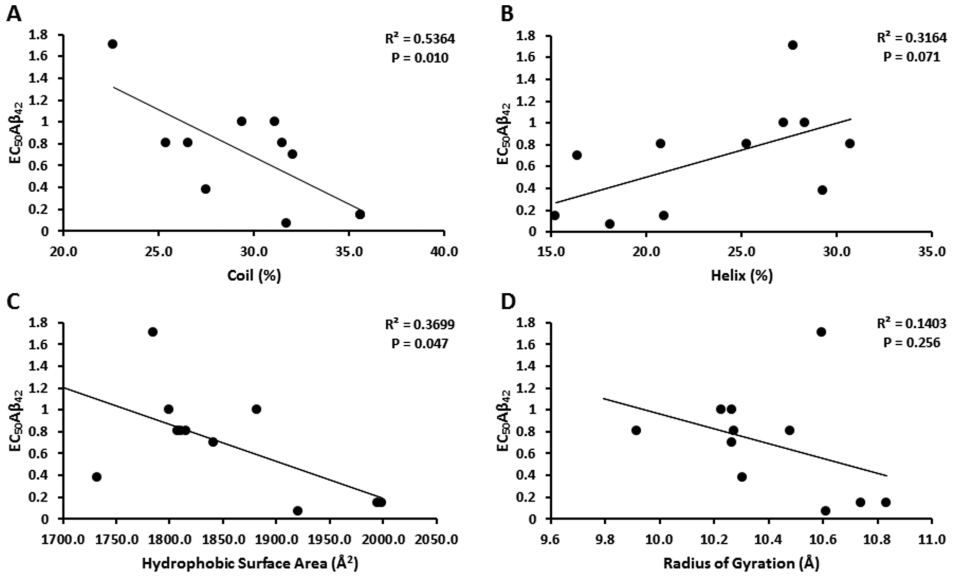

Figure 2. Correlating structural ensembles of amyloid variants directly to experimental toxicity data: (A) vs coil character; (B) vs helix character (C) vs hydrophobic exposure of the ensembles; and (D) vs radius of gyration of the ensembles.

imentally to be most toxic in cell assays. This prompted us to correlate available experimental toxicities of the variants against our computed conformational properties (see below).

We performed a linear regression analysis of the ensemble structural properties the variants, plotted against the relative experimental EC_{50} values of $A\beta_{42}$ variants[18,21,32,38,42] normalized against that of the wild type set to 1 (numerical data in Supporting Information, Table S2). We observed correlations between coil character (R^2 = 0.536, p = 0.010), helix character R^2 = 0.316, p = 0.071), hydrophobic surface area (R^2 = 0.369, p = 0.047), and radius of gyration (R_g) (R^2 = 0.140, p = 0.256) vs experimental cell toxicity (EC_{50}) values of the $A\beta_{42}$ variants (data shown in Figure 2). Furthermore, from outlier analysis, we found that leaving a single data point out substantially increased correlation: D23N was an outlier for helix and hydrophobic surface, whereas A21G was an outlier for R_g. Removal increased R^2 values from 0.316 to 0.472 for helix character, 0.369 to 0.665 for hydrophobic surface, and 0.140 to 0.587 for R_g (Supporting Information, Figure S4). We also note that a corresponding regression analysis against a second experimental toxicity data set for the related $A\beta_{40}$ isoforms gives equally significant correlations for the same structural properties (Supporting Information, Figure S5), further validating our results and indicating that the conformations are central to understanding the relative toxicities of longer vs shorter $A\beta$ isoforms.

Of the four properties that had significant relations to experimental toxicities, helix character showed a positive correlation whereas the remaining properties correlated inversely with corresponding EC_{50} values; that is, helix character relates to reduced toxicity, whereas coil, surface exposure, and conformational size relate to higher toxicity. These observations are qualitatively in agreement with the notion that $\alpha \rightarrow \beta$ transitions are required to form oligomers and that coil and hydrophobic exposure increases the propensity to oligomerize.[30] Our data reveal strong quantitative correlations that offer insight relevant to molecular targeting of the specific conformational features that increase amyloid toxicity. The increased tendency toward helix−coil-strand transition is consistent with an increase in hydrophobic exposure to solvent and increased overall radius of gyration.

The E22 mutants (Arctic, Italian, and Dutch) were found in cell assays to be 10-fold more toxic and the D23N (Iowa) variant 2−3-fold more toxic than wild type $A\beta_{42}$.[19] In contrast, the A21G (Flemish) mutant has been observed to be slightly less cytotoxic than wild type $A\beta_{42}$.[19] These findings are explained by our structural ensembles of the variants, as emphasized more clearly in Figure 3 showing the representative

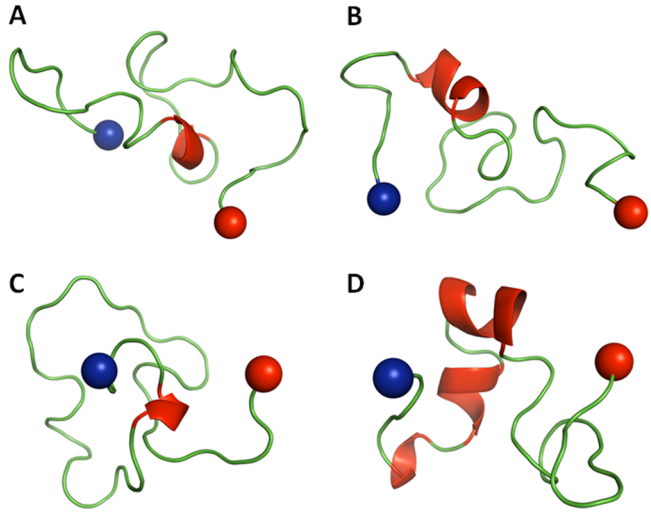

Figure 3. Representative structures for (A) Arctic (E22G), (B) Italian (E22K), (C) Dutch (E22Q), and (D) Iowa (D23N) mutants. Structures were extracted from the most populated clusters of cluster analysis.

(most populated) structures of these four variants. The E22 variants had 32−36% coil character, dropping to 28 and 23% in D23N and A21G. The helix percentage ranged from 15−21% in the E22 variants but increased to 28−29% in A21G and D23N. While the average hydrophobic surface areas of D23N and A21G were 1732 and 1785 Å^2, respectively, the most

DOI: 10.1021/acschemneuro.5b00238
ACS Chem. Neurosci. 2015, 6, 1990−1996

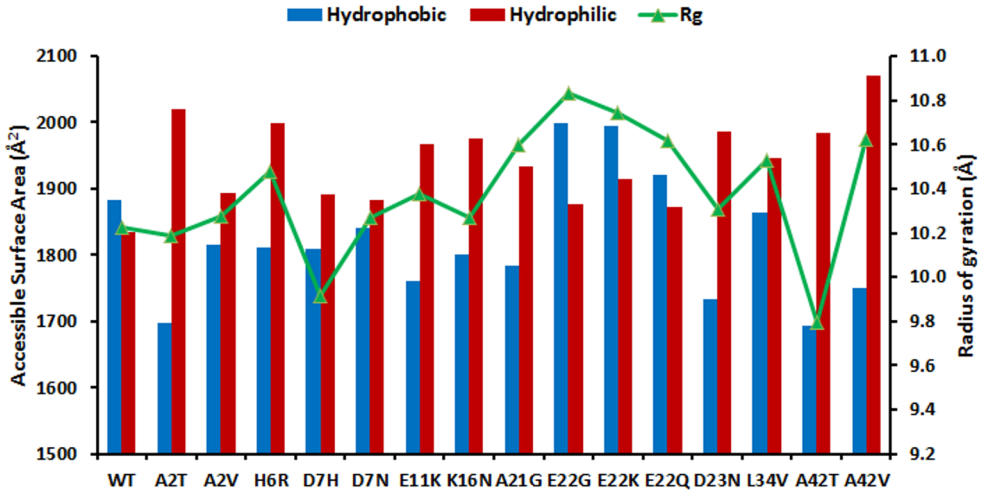

Figure 4. Solvent accessible surface areas and radius of gyration; surface areas were calculated from DSSP program, and radius of gyration was calculated from g_gyrate tool of Gromacs.

pathogenic E22 mutants exhibited substantially increased hydrophobic surface areas of 1920−2000 Å^2.

Specific intermolecular interactions between hydrophobic surfaces of partially folded intermediates are likely to lead to aggregation.[59] Hence, the hydrophobic surface area is an important structural feature of potential pathogenic importance, and we computed this for the ensembles of the studied variants. When compared to wild type 1882 Å^2, the most toxic E22 mutants (Arctic, Italian, and Dutch) had hydrophobic surface areas of 1999, 1995, and 1921 Å^2, respectively, the highest of all variants. The E22 mutants also displayed relatively higher R_g values consistent with more extended and exposed conformations. Interestingly, the protective A2T variant and the late-onset A42T variant displayed the lowest hydrophobic surface areas of 1697 and 1693 Å^2, respectively (Figure 4).

In conclusion, we have reported the first complete comparison of known human genetic variants of Aβ relating to AD and CAA and found that experimental relative toxicities can be largely explained by specific structural features of the variant ensembles. In particular, coil character and hydrophobic exposure, concomitant with reduced helix propensity of the ensembles, provide a statistically significant structure−property relationship for amyloid toxicity and also reveal insight into the protective nature of A2T vs pathogenic A2V. The toxicity of E22 variants is mainly due to increased tendency toward helix−coil-strand transitions, with strand tendencies emerging in the C-terminal of the amyloids known to be critical for oligomerization. The quantitative structural features identified from this study may be relevant to rational design of amyloid-modifying drugs.

METHODS

Structural Models. Aβ is an intrinsically disordered peptide whose secondary structure varies substantially depending on chemical environment.[56] Aβ_{42} is the more pathogenic species likely to seed oligomers, and thus we studied this isoform of the peptide; in addition, many relevant experimental data are available for this isoform. We were interested in the free soluble monomer ensemble as starting point for amyloid processes. There are available crystal structures of Aβ parts cocrystallized with other proteins (e.g., PDB ID: 2G47, 2WK3) and of Aβ multimers. However, no full-length crystal structure of the free Aβ monomer is available, because it is too disordered. Thus, as starting structure we used the published NMR structure of full-length Aβ_{42} with PDB code 1Z0Q.[30] During MD equilibration, the ensembles are equilibrated effectively to different ensembles characteristic of the methods applied, showing that the detailed starting structure is less important.[48] The mutant structures were prepared from the first conformation of 1Z0Q by using protein design extension in Discovery studio 4.0, as described previously.[56]

Simulation Protocol. All the Aβ_{42} structural models that consist of both wild type and mutants were subjected to MD simulation using Gromacs 4.6.7.[60,61] We employed the Amber99sb-ILDN[54] force field, which performed well in our previous force field calibration study on this peptide;[48] its good secondary structure balance, crucial for obtaining a balanced and realistic structural ensemble of Aβ, has also been noted previously.[52−54]

The peptides were initially placed in the center of a cubic box with dimensions 7.1 × 7.1 × 7.1 nm^3 filled with ∼12 020 TIP3P[62] water molecules, the number depending slightly on mutant type. A distance of 1.0 nm was maintained between the protein and the wall of the box to avoid interactions between periodic images. The net negative charge of the system was neutralized by replacing water molecules with Na^+ ions. Additional water molecules were replaced by Na^+ and Cl^- up to 150 mM NaCl to simulate a realistic ionic strength. All the modeled systems were subsequently energy minimized by using the steepest descent algorithm in Gromacs.

To relax the solvent and hydrogen atom positions, the systems were subjected to two-phase position restrained MD. Initially, the system was equilibrated within a canonical NVT ensemble for 100 ps using Berendsen temperature coupling.[63] Subsequent equilibration was carried out in an isothermal−isobaric NPT ensemble for 500 ps using the Nose−Hoover thermostat[64] and Parrinello−Rahman barostat[65] at 300 K and 1 atm. The long-range electrostatic interactions were treated with Particle Mesh Ewald (PME) method.[66] A cutoff of 10 Å was used for Lennard−Jones and Coulomb short-range interactions, and the Linear Constraint Solver (LINCS)[67] algorithm was used to constrain covalent bonds.

To improve stochastic sampling for all mutants and the wild type, all 16 systems were simulated by four independent 100 ns simulations for a total of 400 ns for each system. We clustered the conformations of the ensembles from 20−100 ns of each simulation using a clustering method developed by Daura et al.,[68] based on the backbone atoms and an RMSD cutoff of 3.0 Å.

Analysis of Conformational Properties. The secondary structures were calculated by using the DSSP algorithm.[69] DSSP uses different structural notations during secondary structure determination. We grouped different structural elements into four types: "helix" constitutes α-helix, 3_{10}-helix, and π-helix; "beta" constitutes extended strand and residues in isolated β-bridges; "coil" represents pure coil features; and "turn" represents hydrogen-bonded turns and bends. The top 10 representative structures from clustering

DOI: 10.1021/acschemneuro.5b00238
ACS Chem. Neurosci. 2015, 6, 1990−1996

analysis were used for secondary-structure propensity calculation, weighted by the size (phase space density) of each cluster. To obtain the residue-wise average secondary structures, we combined the four individual trajectories of each variant spanning from 20−100 ns. Secondary structures were calculated for each frame with a frequency gap of 10 ps. The computed properties were correlated against the data set of normalized experimental toxicities previously described.[5]

■ ASSOCIATED CONTENT

Supporting Information

The Supporting Information is available free of charge on the ACS Publications website at DOI: 10.1021/acschemneuro.5b00238.

Figure S1 showing the RMSD plots of the simulations, Figures S2 and S3 showing the residue-based secondary structures of the amyloid variants, Table S1 showing numerical data used in the regression analysis, Table S2 showing the experimental toxicity data normalized to WT, Figure S4 showing the leave-one-out regression analysis, and Figure S5 showing the corresponding analysis using experimental data for the $A\beta_{40}$ isoform (PDF)

■ AUTHOR INFORMATION

Corresponding Author

*E-mail: kpj@kemi.dtu.dk. Phone: +045 45 25 24 09.

Funding

The Danish Council for Independent Research | Natural sciences (FNU) (grant ID: DFF − 1323-00110B) and the Danish Center for Scientific Computing (grant ID: 2012-02-23) are acknowledged for supporting this work.

Notes

The authors declare no competing financial interest.

■ REFERENCES

(1) Nasica-Labouze, J., Nguyen, P. H., Sterpone, F., Berthoumieu, O., Buchete, N.-V., Coté, S., De Simone, A., Doig, A. J., Faller, P., Garcia, A., Laio, A., Li, M. S., Melchionna, S., Mousseau, N., Mu, Y., Paravastu, A., Pasquali, S., Rosenman, D. J., Strodel, B., Tarus, B., Viles, J. H., Zhang, T., Wang, C., and Derreumaux, P. (2015) Amyloid β Protein and Alzheimer's Disease: When Computer Simulations Complement Experimental Studies. *Chem. Rev. 115*, 3518−3563.

(2) Kepp, K. P. (2012) Bioinorganic chemistry of Alzheimer's disease. *Chem. Rev. 112*, 5193−5239.

(3) Hardy, J., and Selkoe, D. J. (2002) The amyloid hypothesis of Alzheimer's disease: progress and problems on the road to therapeutics. *Science 297*, 353−356.

(4) Eisenberg, D., and Jucker, M. (2012) The amyloid state of proteins in human diseases. *Cell 148*, 1188−1203.

(5) Tiwari, M. K., and Kepp, K. P. (2015) Modeling the Aggregation Propensity and Toxicity of Amyloid-β Variants. *J. Alzheimer's Dis. 47*, 215−229.

(6) De Strooper, B., Saftig, P., Craessaerts, K., Vanderstichele, H., Guhde, G., Annaert, W., Von Figura, K., and Van Leuven, F. (1998) Deficiency of presenilin-1 inhibits the normal cleavage of amyloid precursor protein. *Nature 391*, 387−390.

(7) Haass, C., and Selkoe, D. J. (1998) Alzheimer's disease. A technical KO of amyloid-beta peptide. *Nature 391*, 339−340.

(8) Karran, E., Mercken, M., and De Strooper, B. (2011) The amyloid cascade hypothesis for Alzheimer's disease: an appraisal for the development of therapeutics. *Nat. Rev. Drug Discovery 10*, 698−712.

(9) Kayed, R., Head, E., Thompson, J. L., McIntire, T. M., Milton, S. C., Cotman, C. W., and Glabe, C. G. (2003) Common structure of soluble amyloid oligomers implies common mechanism of pathogenesis. *Science 300*, 486−489.

(10) Sciacca, M. F. M., Kotler, S. A., Brender, J. R., Chen, J., Lee, D. K., and Ramamoorthy, A. (2012) Two-step mechanism of membrane disruption by Aβ through membrane fragmentation and pore formation. *Biophys. J. 103*, 702−710.

(11) Ramamoorthy, A., and Lim, M. H. (2013) Structural characterization and inhibition of toxic amyloid-β oligomeric intermediates. *Biophys. J. 105*, 287−288.

(12) Savelieff, M. G., Liu, Y., Senthamarai, R. R. P., Korshavn, K. J., Lee, H. J., Ramamoorthy, A., and Lim, M. H. (2014) A small molecule that displays marked reactivity toward copper- versus zinc-amyloid-β implicated in Alzheimer's disease. *Chem. Commun. 50*, 5301−5303.

(13) Hendriks, L., van Duijn, C. M., Cras, P., Cruts, M., Van Hul, W., van Harskamp, F., Warren, A., McInnis, M. G., Antonarakis, S. E., Martin, J. J., et al. (1992) Presenile dementia and cerebral haemorrhage linked to a mutation at codon 692 of the beta-amyloid precursor protein gene. *Nat. Genet. 1*, 218−221.

(14) Kamino, K., Orr, H. T., Payami, H., Wijsman, E. M., Alonso, M. E., Pulst, S. M., Anderson, L., O'dahl, S., Nemens, E., and White, J. A. (1992) Linkage and mutational analysis of familial Alzheimer disease kindreds for the APP gene region. *Am. J. Hum. Genet. 51*, 998−1014.

(15) Rossi, G., Macchi, G., Porro, M., Giaccone, G., Bugiani, M., Scarpini, E., Scarlato, G., Molini, G. E., Sasanelli, F., Bugiani, O., and Tagliavini, F. (1998) Fatal familial insomnia: genetic, neuropathologic, and biochemical study of a patient from a new Italian kindred. *Neurology 50*, 688−692.

(16) Van Broeckhoven, C., Haan, J., Bakker, E., Hardy, J. A., Van Hul, W., Wehnert, A., Vegter-Van der Vlis, M., and Roos, R. A. (1990) Amyloid beta protein precursor gene and hereditary cerebral hemorrhage with amyloidosis (Dutch). *Science 248*, 1120−1122.

(17) Grabowski, T. J., Cho, H. S., Vonsattel, J. P., Rebeck, G. W., and Greenberg, S. M. (2001) Novel amyloid precursor protein mutation in an Iowa family with dementia and severe cerebral amyloid angiopathy. *Ann. Neurol. 49*, 697−705.

(18) Nilsberth, C., Westlind-Danielsson, A., Eckman, C. B., Condron, M. M., Axelman, K., Forsell, C., Stenh, C., Luthman, J., Teplow, D. B., Younkin, S. G., Näslund, J., and Lannfelt, L. (2001) The "Arctic" APP mutation (E693G) causes Alzheimer's disease by enhanced Abeta protofibril formation. *Nat. Neurosci. 4*, 887−893.

(19) Murakami, K., Irie, K., Morimoto, A., Ohigashi, H., Shindo, M., Nagao, M., Shimizu, T., and Shirasawa, T. (2003) Neurotoxicity and physicochemical properties of Aβ mutant peptides from cerebral amyloid angiopathy: Implication for the pathogenesis of cerebral amyloid angiopathy and Alzheimer's disease. *J. Biol. Chem. 278*, 46179−46187.

(20) Janssen, J. C., Beck, J. A., Campbell, T. A., Dickinson, A., Fox, N. C., Harvey, R. J., Houlden, H., Rossor, M. N., and Collinge, J. (2003) Early onset familial Alzheimer's disease: Mutation frequency in 31 families. *Neurology 60*, 235−239.

(21) Chen, W. T., Hong, C. J., Lin, Y. T., Chang, W. H., Huang, H. T., Liao, J. Y., Chang, Y. J., Hsieh, Y. F., Cheng, C. Y., Liu, H. C., Chen, Y. R., and Cheng, I. H. (2012) Amyloid-beta (Aβ) D7H mutation increases oligomeric Aβ42 and alters properties of Aβ-zinc/copper assemblies. *PLoS One 7*, e35807.

(22) Wakutani, Y., Watanabe, K., Adachi, Y., Wada-Isoe, K., Urakami, K., Ninomiya, H., Saido, T. C., Hashimoto, T., Iwatsubo, T., and Nakashima, K. (2004) Novel amyloid precursor protein gene missense mutation (D678N) in probable familial Alzheimer's disease. *J. Neurol., Neurosurg. Psychiatry 75*, 1039−1042.

(23) Hori, Y., Hashimoto, T., Wakutani, Y., Urakami, K., Nakashima, K., Condron, M. M., Tsubuki, S., Saido, T. C., Teplow, D. B., and Iwatsubo, T. (2007) The Tottori (D7N) and English (H6R) familial Alzheimer disease mutations accelerate Aβ fibril formation without increasing protofibril formation. *J. Biol. Chem. 282*, 4916−4923.

(24) Tseng, B. P., Esler, W. P., Clish, C. B., Stimson, E. R., Ghilardi, J. R., Vinters, H. V., Mantyh, P. W., Lee, J. P., and Maggio, J. E. (1999) Deposition of monomeric, not oligomeric, Abeta mediates growth of

DOI: 10.1021/acschemneuro.5b00238
ACS Chem. Neurosci. 2015, 6, 1990−1996

Alzheimer's disease amyloid plaques in human brain preparations. *Biochemistry 38*, 10424−31.
(25) Shankar, G. M., Li, S., Mehta, T. H., Garcia-Munoz, A., Shepardson, N. E., Smith, I., Brett, F. M., Farrell, M. a, Rowan, M. J., Lemere, C. a, Regan, C. M., Walsh, D. M., Sabatini, B. L., and Selkoe, D. J. (2008) Amyloid-beta protein dimers isolated directly from Alzheimer's brains impair synaptic plasticity and memory. *Nat. Med. 14*, 837−842.
(26) Klyubin, I., Betts, V., Welzel, a. T., Blennow, K., Zetterberg, H., Wallin, a., Lemere, C. a., Cullen, W. K., Peng, Y., Wisniewski, T., Selkoe, D. J., Anwyl, R., Walsh, D. M., and Rowan, M. J. (2008) Amyloid Protein Dimer-Containing Human CSF Disrupts Synaptic Plasticity: Prevention by Systemic Passive Immunization. *J. Neurosci. 28*, 4231−4237.
(27) Nag, S., Sarkar, B., Bandyopadhyay, A., Sahoo, B., Sreenivasan, V. K. a., Kombrabail, M., Muralidharan, C., and Maiti, S. (2011) Nature of the Amyloid-β Monomer and the Monomer-Oligomer Equilibrium. *J. Biol. Chem. 286*, 13827−13833.
(28) Giuffrida, M. L., Caraci, F., De Bona, P., Pappalardo, G., Nicoletti, F., Rizzarelli, E., and Copani, a. (2010) The Monomer State of β-Amyloid: Where the Alzheimer's Disease protein Meets Physiology. *Rev. Neurosci. 21*, 83−93.
(29) Bernstein, S. L., Wyttenbach, T., Baumketner, A., Shea, J.-E., Bitan, G., Teplow, D. B., and Bowers, M. T. (2005) Amyloid beta-protein: monomer structure and early aggregation states of Abeta42 and its Pro19 alloform. *J. Am. Chem. Soc. 127*, 2075−2084.
(30) Tomaselli, S., Esposito, V., Vangone, P., Van Nuland, N. A. J., Bonvin, A. M. J. J., Guerrini, R., Tancredi, T., Temussi, P. A., and Picone, D. (2006) The α-to-β conformational transition of Alzheimer's Aβ-(1−42) peptide in aqueous media is reversible: A step by step conformational analysis suggests the location of β conformation seeding. *ChemBioChem 7*, 257−267.
(31) Ahmed, M., Davis, J., Aucoin, D., Sato, T., Ahuja, S., Aimoto, S., Elliott, J. I., Van Nostrand, W. E., and Smith, S. O. (2010) Structural conversion of neurotoxic amyloid-β1−42 oligomers to fibrils. *Nat. Struct. Mol. Biol. 17*, 561−567.
(32) Ono, K., Condron, M. M., and Teplow, D. B. (2010) Effects of the english (H6R) and tottori (D7N) familial alzheimer disease mutations on amyloid β-protein assembly and toxicity. *J. Biol. Chem. 285*, 23186−23197.
(33) Xu, L., Shan, S., and Wang, X. (2013) Single point mutation alters the microstate dynamics of amyloid β-protein Aβ42 as revealed by dihedral dynamics analyses. *J. Phys. Chem. B 117*, 6206−6216.
(34) Peacock, M. L., Warren, J. T., Roses, A. D., and Fink, J. K. (1993) Novel polymorphism in the A4 region of the amyloid precursor protein gene in a patient without Alzheimer's disease. *Neurology 43*, 1254−1256.
(35) Qahwash, I., Weiland, K. L., Lu, Y., Sarver, R. W., Kletzien, R. F., and Yan, R. (2003) Identification of a mutant amyloid peptide that predominantly forms neurotoxic protofibrillar aggregates. *J. Biol. Chem. 278*, 23187−23195.
(36) Jonsson, T., Atwal, J. K., Steinberg, S., Snaedal, J., Jonsson, P. V., Bjornsson, S., Stefansson, H., Sulem, P., Gudbjartsson, D., Maloney, J., Hoyte, K., Gustafson, A., Liu, Y., Lu, Y., Bhangale, T., Graham, R. R., Huttenlocher, J., Bjornsdottir, G., Andreassen, O. A., Jönsson, E. G., Palotie, A., Behrens, T. W., Magnusson, O. T., Kong, A., Thorsteinsdottir, U., Watts, R. J., and Stefansson, K. (2012) A mutation in APP protects against Alzheimer's disease and age-related cognitive decline. *Nature 488*, 96−99.
(37) Benilova, I., Gallardo, R., Ungureanu, A.-A., Castillo Cano, V., Snellinx, A., Ramakers, M., Bartic, C., Rousseau, F., Schymkowitz, J., and De Strooper, B. (2014) The Alzheimer disease protective mutation A2T modulates kinetic and thermodynamic properties of amyloid-β (Aβ) aggregation. *J. Biol. Chem. 289*, 30977−30989.
(38) Di Fede, G., Catania, M., Morbin, M., Rossi, G., Suardi, S., Mazzoleni, G., Merlin, M., Giovagnoli, A. R., Prioni, S., Erbetta, A., Falcone, C., Gobbi, M., Colombo, L., Bastone, A., Beeg, M., Manzoni, C., Francescucci, B., Spagnoli, A., Cantù, L., Del Favero, E., Levy, E., Salmona, M., and Tagliavini, F. (2009) A recessive mutation in the APP gene with dominant-negative effect on amyloidogenesis. *Science 323*, 1473−1477.
(39) Obici, L., Demarchi, A., de Rosa, G., Bellotti, V., Marciano, S., Donadei, S., Arbustini, E., Palladini, G., Diegoli, M., Genovese, E., Ferrari, G., Coverlizza, S., and Merlini, G. (2005) A novel AβPP mutation exclusively associated with cerebral amyloid angiopathy. *Ann. Neurol. 58*, 639−644.
(40) Brouwers, N., Sleegers, K., and Van Broeckhoven, C. (2008) Molecular genetics of Alzheimer's disease: an update. *Ann. Med. 40*, 562−583.
(41) Zhou, L., Brouwers, N., Benilova, I., Vandersteen, A., Mercken, M., Van Laere, K., Van Damme, P., Demedts, D., Van Leuven, F., Sleegers, K., Broersen, K., Van Broeckhoven, C., Vandenberghe, R., and De Strooper, B. (2011) Amyloid precursor protein mutation E682K at the alternative β-secretase cleavage β'-site increases Aβ generation. *EMBO Mol. Med. 3*, 291−302.
(42) Kaden, D., Harmeier, A., Weise, C., Munter, L. M., Althoff, V., Rost, B. R., Hildebrand, P. W., Schmitz, D., Schaefer, M., Lurz, R., Skodda, S., Yamamoto, R., Arlt, S., Finckh, U., and Multhaup, G. (2012) Novel APP/Aβ mutation K16N produces highly toxic heteromeric Aβ oligomers. *EMBO Mol. Med. 4*, 647−659.
(43) Bernardi, L., Geracitano, S., Colao, R., Puccio, G., Gallo, M., Anfossi, M., Frangipane, F., Curcio, S. A. M., Mirabelli, M., Tomaino, C., Vasso, F., Smirne, N., Maletta, R., and Bruni, A. C. (2009) AβPP A713T mutation in late onset alzheimer's disease with cerebrovascular lesions. *J. Alzheimer's Dis. 17*, 383−389.
(44) Jones, C. T., Morris, S., Yates, C. M., Moffoot, A., Sharpe, C., Brock, D. J. H., and St. Clair, D. (1992) Mutation in codon 713 of the β amyloid precursor protein gene presenting with schizophrenia. *Nat. Genet. 1*, 306−309.
(45) Forsell, C., and Lannfelt, L. (1995) Amyloid precursor protein mutation at codon 713 (Ala– > Val) does not cause schizophrenia: non-pathogenic variant found at codon 705 (silent). *Neurosci. Lett. 184*, 90−93.
(46) Choi, J.-S., Braymer, J. J., Nanga, R. P. R., Ramamoorthy, A., and Lim, M. H. (2010) Design of small molecules that target metal-Aβ species and regulate metal-induced Aβ aggregation and neurotoxicity. *Proc. Natl. Acad. Sci. U. S. A. 107*, 21990−21995.
(47) Hindo, S. S., Mancino, A. M., Braymer, J. J., Liu, Y., Vivekanandan, S., Ramamoorthy, A., and Lim, M. H. (2009) Small molecule modulators of copper-induced Aβ aggregation. *J. Am. Chem. Soc. 131*, 16663−16665.
(48) Somavarapu, A. K., and Kepp, K. P. (2015) The Dependence of Amyloid-β Dynamics on Protein Force Fields and Water Models. *ChemPhysChem*, DOI: 10.1002/cphc.201500415.
(49) Das, P., Kang, S., Temple, S., and Belfort, G. (2014) Interaction of amyloid inhibitor proteins with amyloid beta peptides: insight from molecular dynamics simulations. *PLoS One 9*, e113041.
(50) Kříž, Z., Klusák, J., Krištofíková, Z., and Koča, J. (2013) How ionic strength affects the conformational behavior of human and rat beta amyloids–a computational study. *PLoS One 8*, e62914.
(51) Hernández-Rodríguez, M., Correa-Basurto, J., Benitez-Cardoza, C. G., Resendiz-Albor, A. A., and Rosales-Hernández, M. C. (2013) In silico and in vitro studies to elucidate the role of Cu2+ and galanthamine as the limiting step in the amyloid beta (1−42) fibrillation process. *Protein Sci. 22*, 1320−1335.
(52) Cino, E. A., Choy, W., and Karttunen, M. (2012) Comparison of Secondary Structure Formation Using 10 Di ff erent Force Fields in Microsecond Molecular Dynamics Simulations. *J. Chem. Theory Comput. 8*, 2725−2740.
(53) Beauchamp, K. A., Lin, Y.-S., Das, R., and Pande, V. S. (2012) Are Protein Force Fields Getting Better? A Systematic Benchmark on 524 Diverse NMR Measurements. *J. Chem. Theory Comput. 8*, 1409−1414.
(54) Lindorff-Larsen, K., Piana, S., Palmo, K., Maragakis, P., Klepeis, J. L., Dror, R. O., and Shaw, D. E. (2010) Improved side-chain torsion potentials for the Amber ff99SB protein force field. *Proteins: Struct., Funct., Bioinf. 78*, 1950−1958.

DOI: 10.1021/acschemneuro.5b00238
ACS Chem. Neurosci. 2015, 6, 1990−1996

(55) Vivekanandan, S., Brender, J. R., Lee, S. Y., and Ramamoorthy, A. (2011) A partially folded structure of amyloid-β(1−40) in an aqueous environment. *Biochem. Biophys. Res. Commun. 411*, 312−316.
(56) Tiwari, M. K., and Kepp, K. P. (2015) Pathogenic properties of Alzheimer's β-amyloid identified from structure−property patient-phenotype correlations. *Dalt. Trans. 44*, 2747−2754.
(57) Crescenzi, O., Tomaselli, S., Guerrini, R., Salvadori, S., D'Ursi, A. M., Temussi, P. A., and Picone, D. (2002) Solution structure of the Alzheimer amyloid β-peptide (1−42) in an apolar microenvironment: Similarity with a virus fusion domain. *Eur. J. Biochem. 269*, 5642−5648.
(58) Coles, M., Bicknell, W., Watson, A. A., Fairlie, D. P., and Craik, D. J. (1998) Solution structure of amyloid beta-peptide(1−40) in a water-micelle environment. Is the membrane-spanning domain where we think it is? *Biochemistry 37*, 11064−77.
(59) Fink, A. L. (1998) Protein aggregation: folding aggregates, inclusion bodies and amyloid. *Folding Des. 3*, R9−23.
(60) Pronk, S., Páll, S., Schulz, R., Larsson, P., Bjelkmar, P., Apostolov, R., Shirts, M. R., Smith, J. C., Kasson, P. M., Van Der Spoel, D., Hess, B., and Lindahl, E. (2013) GROMACS 4.5: A high-throughput and highly parallel open source molecular simulation toolkit. *Bioinformatics 29*, 845−854.
(61) Hess, B., Kutzner, C., van der Spoel, D., and Lindahl, E. (2008) GROMACS 4: Algorithms for Highly Efficient, Load-Balanced, and Scalable Molecular Simulation. *J. Chem. Theory Comput. 4*, 435−447.
(62) Jorgensen, W. L., Chandrasekhar, J., Madura, J. D., Impey, R. W., and Klein, M. L. (1983) Comparison of simple potential functions for simulating liquid water. *J. Chem. Phys. 79*, 926.
(63) Berendsen, H. J. C., Postma, J. P. M., van Gunsteren, W. F., DiNola, A., and Haak, J. R. (1984) Molecular dynamics with coupling to an external bath. *J. Chem. Phys. 81*, 3684.
(64) Nosé, S., and Klein, M. L. (1983) Constant pressure molecular dynamics for molecular systems. *Mol. Phys. 50*, 1055−1076.
(65) Parrinello, M., and Rahman, A. (1981) Polymorphic Transitions in Single Crystals: a New Molecular Dynamics Method. *J. Appl. Phys. 52*, 7182−7190.
(66) Darden, T., York, D., and Pedersen, L. (1993) Particle mesh Ewald: An N·log(N) method for Ewald sums in large systems. *J. Chem. Phys. 98*, 10089.
(67) Hess, B. (2008) P-LINCS: A Parallel Linear Constraint Solver for Molecular Simulation. *J. Chem. Theory Comput. 4*, 116−122.
(68) Daura, X., Gademann, K., Jaun, B., Seebach, D., van Gunsteren, W. F., and Mark, A. E. (1999) Peptide Folding: When Simulation Meets Experiment. *Angew. Chem., Int. Ed. 38*, 236−240.
(69) Kabsch, W., and Sander, C. (1983) Dictionary of protein secondary structure: pattern recognition of hydrogen-bonded and geometrical features. *Biopolymers 22*, 2577−2637.

DOI: 10.1021/acschemneuro.5b00238
ACS Chem. Neurosci. 2015, 6, 1990−1996